Proceedings of FEDSM2006
2006 ASME Joint U.S. - European Fluids Engineering Summer Meeting
July 17-20, Miami, FL

FEDSM2006-98399

NUMERICAL SIMULATION AND EXPERIMENTS OF THE MULTIPHASE FLOW IN A LIQUID-LIQUID CYLINDRICAL CYCLONE SEPARATOR

Miguel A Reyes
Universidad Simón Bolívar, Caracas, Venezuela. Dpto. de Termodinámica y Fenómenos de Transferencia. mareyes@usb.ve

Jorge E Pacheco
Universidad Simón Bolívar, Caracas, Venezuela. Dpto. de Termodinámica y Fenómenos de Transferencia. jorgepacheco@usb.ve

Juan C Marín
Universidad Simón Bolívar, Caracas, Venezuela. CEMFA

Luis R Rojas
Universidad Simón Bolívar, Caracas, Venezuela. Dpto. de Conversión y Transporte de Energía. rrojas@usb.ve

José Rincón
Universidad del Zulia, Maracaibo, Venezuela. Facultad de Ingeniería. Dpto. de Energía

ABSTRACT

A Liquid-Liquid Cylindrical Cyclone separator (LLCC) is a device used in the petroleum industry to separate the oil-water mixture obtained from the well. The use of this device has not been widespread due to the lack of tools for predicting its separation capability. This paper presents a numerical and experimental study of the fluid dynamic performance of this type of cylindrical cyclone separators. The use of numerical simulations would reduce the time and cost necessary to obtain information for predicting the behavior of the equipment. The objective of this study is to determine if CFD (Computational Fluid Dynamics) techniques are able to reproduce the behavior of a LLCC separator. The CFD software examined was ANSYS-CFX 5.6™ and numerical simulations were carried out using the dispersed model with oil as the dispersed phase. The oil and water mixture entering the separator is divided due to centrifugal and buoyancy forces in an upper (oil rich) exit and a bottom (water rich) exit. The separation capability is determined as the maximum amount of water removed from the mixture with the minimum amount of oil content in the water rich exit. The experiments were conducted in a transparent LLCC separator that allows the visualization of the mixture and the measurement of the oil content. Experiments were conducted for three variables: mixture velocity and water content at the entrance, and the split ratio. The split ratio is defined as the bottom exit flow rate divided by the water flow rate at the entrance. The results showed that CFD tools are able to reproduce the oil content obtained from the experiments for all analyzed conditions. Additionally, the mixture distribution images from numerical and experimental data showed good agreement. This study confirms the capacity of CFD tools for the multiphase flow analysis of LLCC separators.

Keywords: Multiphase flow, numerical simulation, separator, oil-water, cyclone.

INTRODUCTION

It is common in the oil industry to extract oil as a mixture with high water content. In these situations it would be beneficial to reduce the amount of water in the mixture, near the well, in order to reduce pumping costs and the size of downstream equipments. For this purpose LLCC (Liquid Liquid Cylindrical Cyclone) separators have been designed. These devices are low-cost, space-saving and low-maintenance when compared with conventional vessel type separators. However the inability to predict its performance adequately has hindered its widespread use [1].

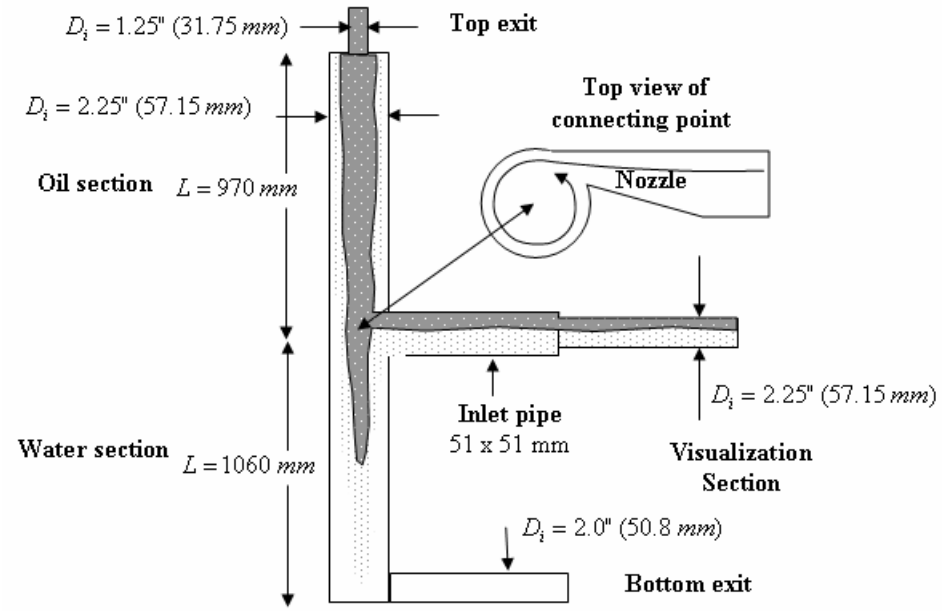

Figure 1. Dimensions of the LLCC separator.

Cylindrical cyclones have been extensively studied for liquid-gas separation. For example, mechanistic models have been successfully developed from experimental data fitting and physical derivation [2], while full 3D CFD studies have been performed in order to further the understanding of the complex flow within this separator [3, 4]. Therefore, even though experiments and mechanistic models provide a useful tool for GLCC (Gas Liquid Cylindrical Cyclone) development, it is well recognized the important role of CFD as a mean for studying the turbulence and flow field within the separator and therefore, a very powerful tool to improving existent correlations and mechanistic models.

Alternatively, research has been carried out to study the LLCC behavior [5] or to develop simulators [6] and control systems [7]. These separators although not able to separate both phases (oil and water) completely, can extract a good portion of the water with very low oil content The use of LLCC separators has been limited by the lack of mathematical models that can predict their behavior. In fact, despite the usefulness of the CFD techniques, previous studies of the LLCC have been based on collection of experimental data and development of mechanistic models that incorporate the physical phenomena. CFD techniques have been avoided for the study of the LLCC because of the extensive work associated with it [8].

The objective of this work is to determine if available state-of-the-art CFD tools can be reasonably used to predict the centrifugal separation process and the magnitude of the oil carry-under. The use of numerical simulations would reduce significantly the resources spent on experiments and could help developed simpler mathematical models.

The LLCC separator consists of a vertical cylinder, which connects to a horizontal pipe around its midpoint (See Fig. 1). The horizontal pipe includes a nozzle at the connecting point with the vertical cylinder that accelerates the mixture and creates the desired centrifugal force. The mixture is separated by the centrifugal force within the vertical cylinder; the water free of oil leaves through the bottom exit, also called water leg, while the rest of the mixture (rich in oil) leaves through the top exit, also called oil leg. The dimensions of the separator used for the experiments and numerical simulations are shown in Fig 1.

MATHEMATICAL MODEL

The governing equations for the turbulent two-phase flow under an Eulerian-Eulerian non-homogeneous scheme are shown in Table 1.

Table 1. Governing Equations

Momentum	$\nabla \bullet \left(r_\alpha \left(\rho_\alpha U_\alpha \otimes U_\alpha - \mu_\alpha \left(\nabla U_\alpha + (\nabla U_\alpha)^T \right) \right) \right) = r_\alpha (B - \nabla p_\alpha) + \sum_{\beta=1}^{N_P} c_{\alpha\beta}^{(d)} (U_\beta - U_\alpha)$ **(1)**		
Exchange of Momentum between Phases	$c_{\alpha\beta}^{(d)} = \frac{3}{4} \frac{C_D}{d} r_\beta \rho_\alpha \lvert U_\beta - U_\alpha \rvert$ **(2a)**	$C_{D(sphere)} = \frac{24}{\mathrm{Re}} \left(1 + 0.1\ \mathrm{Re}^{0.75}\right)$ **(2b)**	$C_D = r_c^{\,p} C_{D(sphere)}$ **(2c)**
Continuity	$\nabla \bullet \left(r_\alpha \rho_\alpha U_\alpha \right) = 0$ **(3)**		
Turbulent Kinetic Energy	$\frac{\partial}{\partial t} \left(r_\alpha \rho_\alpha k_\alpha \right) + \nabla \bullet \left(r_\alpha \left(\rho_\alpha U_\alpha k_\alpha - \left(\mu + \frac{\mu_{T\alpha}}{\sigma_k} \right) \nabla k_\alpha \right) \right) = r_\alpha S_{k\alpha}$ **(4)**		
Turbulent Dissipation and Prandtl-Kolmogorov relation for μ_T, k and ε	$\frac{\partial}{\partial t} \left(r_\alpha \rho_\alpha \varepsilon_\alpha \right) + \nabla \bullet \left(r_\alpha \left(\rho_\alpha U_\alpha \varepsilon_\alpha - \left(\mu + \frac{\mu_{T\alpha}}{\sigma_\varepsilon} \right) \nabla \varepsilon_\alpha \right) \right) = r_\alpha S_{\varepsilon\alpha}$ **(5)**		
	$\mu_T = C_\mu \rho \frac{k^2}{\varepsilon}$, $S_{k\alpha} = P_\alpha + G_\alpha - \rho_\alpha \varepsilon_\alpha$, $S_{\varepsilon\alpha} = \frac{\varepsilon_\alpha}{k_\alpha} \left(C_{1\varepsilon} \left(P_\alpha + C_{3\varepsilon} \max(G_\alpha, 0) \right) - C_{2\varepsilon} \rho_\alpha \varepsilon_\alpha \right)$		

The subscripts α and β denote the different phases contained in the domain. The convective terms, diffusive terms and body forces of the momentum conservation equation are multiplied by the volumetric fraction of the corresponding phase because each one occupies only one fraction of the considered space. The exchange of momentum between the α and β phases is included as a source term and it is calculated assuming the presence of a continuous phase and a dispersed phase, in the form of drops. For spherical drops, the $c^{(d)}_{\alpha\beta}$ term reduces to Eq. 2a. Grace's drag [9] model is used, which calculates the drag coefficient through Eq. 2b and corrects it with a factor that depends on the concentration of the continuous phase according to Eq. 2c. The volumetric fraction of the continuous phase is denoted as r_c and the empirical coefficient is denoted as p. Eq. 2c reduces the drag coefficient as the concentration of drops increases.

Properties k and ε necessary to calculate the turbulent viscosity are obtained by equations 4 and 5. CFX 5.6 ™ uses the control volumes based finite element method (CVFEM) with either structured or non-structured meshes, according to the user criterion. This software uses tetrahedral, hexagonal and prismatic elements to discretize the differential equations and a non-segregated method to couple momentum and continuity equations.

NUMERICAL SIMULATIONS

The mesh used in the simulations consists of 221507 elements and 66757 nodes with mesh refinements at the entrance, nozzle and the injection area as shown in Fig. 2. Previous studies determined that this amount of nodes is sufficient to obtain a mesh-independent solution [10].

Boundary conditions of stratified flow at the entrance, flow rate at the water leg and pressure at the oil leg were specified. An oil drop diameter of 1 mm was empirically obtained by matching experimental data and numerical results at one particular condition (v_m=0.375 m/s, S=0.7). The rest of the simulations were performed using the same oil drop diameter. This oil drop diameter is in good agreement with experimental data, shown in [11], obtained at similar mixture velocities. The RNG κ-ε turbulence model was used since it has shown satisfactory results when comparing the speed of rotation of the mixture with experimental data [10]. The simulation runs were carried out in a Pentium IV 3.2 GHz, 1 GB RAM computer taking approximately 5 hours for each run.

EXPERIMENTS DESCRIPTION

The experiments were conducted in a multiphase flow facility designed and constructed in the Centro de Mecánica de Fluidos y Aplicaciones (CEMFA) of Universidad Simón Bolívar. The working fluids were water and oil (PDV-PUROLUB 46) whose density and viscosity at 20ºC are 870 kg/m^3 and 130 cP, respectively. This oil is equivalent to a 22 º API crude oil. The experimental facility is shown in Fig. 3.

The measured variables are: oil flow rate at the entrance, water flow rate at the entrance, flow rate and the volumetric fraction of oil (VFo) at the water leg. The volumetric fraction of oil at the water leg is obtained by taking a 4-liter sample of the mixture. This sample is left resting for at least 24 hours, then the oil is extracted with a pipette and its volume is divided by the total volume of the sample. Experiments with water percentages of 60, 75 and 90 %, and with mixture velocities (v_m) at the entrance of the separator of 0.25, 0.375 and 0.5 m/s were conducted.

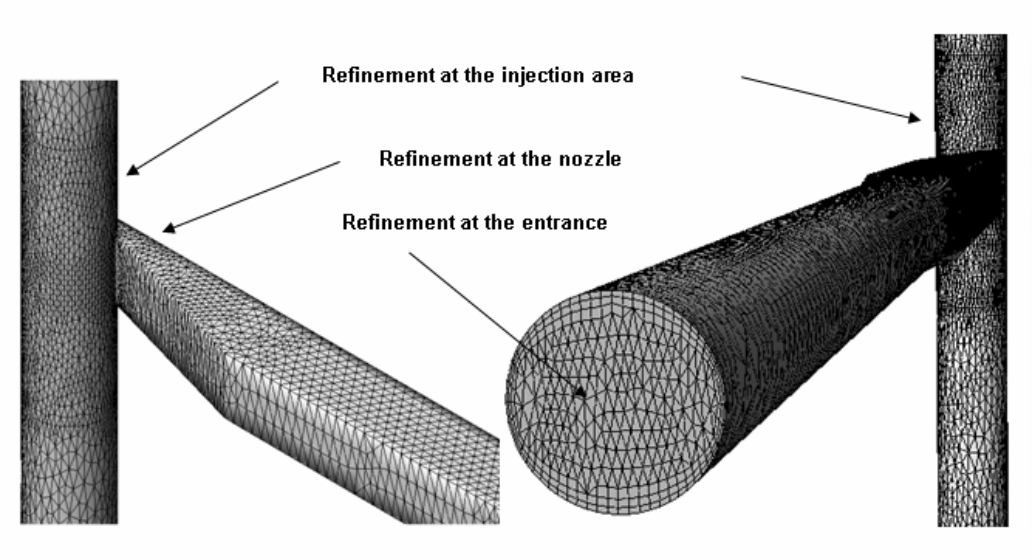

Figure 2. Areas with mesh refinement.

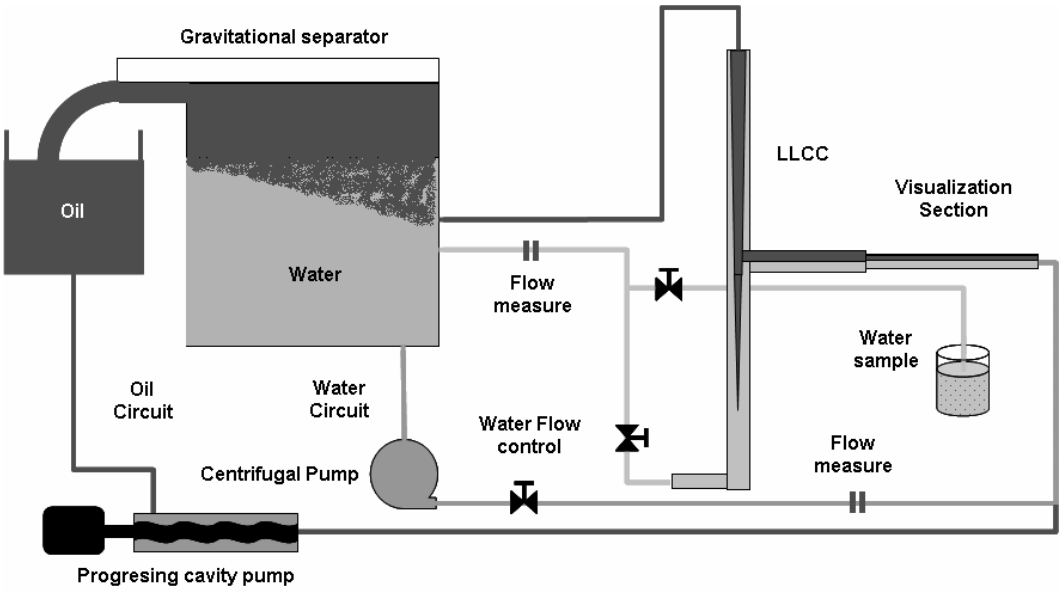

Figure 3. Multiphase flow facility

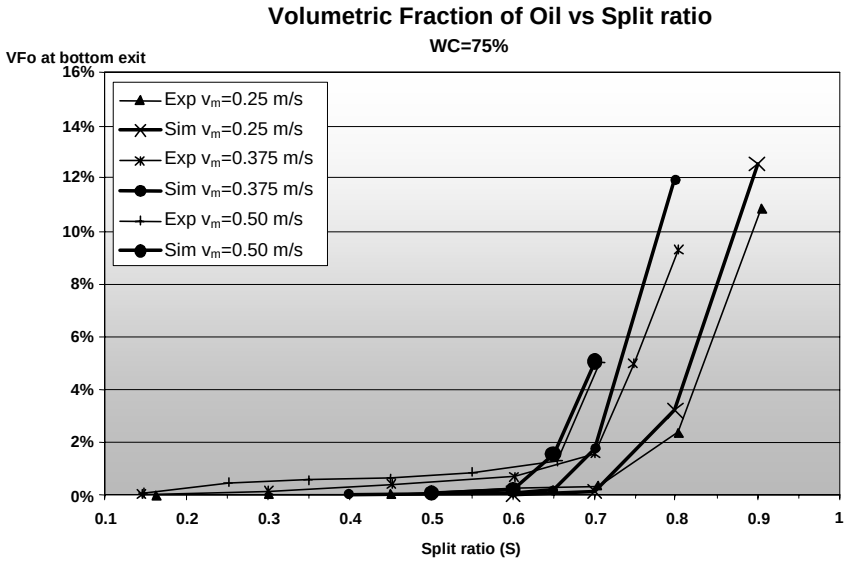

Figure 4. Volumetric Fraction of Oil (VFo) at water leg versus Split ratio (S) for a mixture with 75% water.

RESULTS

Figure 4 shows the comparison between numerical simulations and experiments for VFo at water leg versus split ratio (S). The split ratio is defined as the bottom exit flow rate divided by the water flow rate at the entrance. This figure shows results for a mixture with 75% water content (wc) at the entrance and mixture velocity (v_m) of 0.25, 0.375 and 0.5 m/s. Under an ideal separation process, the maximum split ratio that could be obtained for a 100% watercut at the water leg would be of one (S = 1). However, since the separation process is not ideal, oil drag usually happens with split ratios smaller than one. Optimal Split Ratio (OSR) is defined as the maximum value before oil drag occurs through the water leg. In figure 4, the observed OSR is between 0.6 and 0.7. This means that the maximum amount of water that can be removed with this device in these operating conditions before oil is dragged is between 60% and 70%.

Agreement between numerical simulation and experimental results is satisfactory, in particular with respect to OSR values. Similar results were obtained for mixtures with 60 % and 90 % water content, which are omitted for space reasons.

Below the OSR for v_m of 0.375 and 0.5 m/s, the experiments showed a quite small oil drag (VFo < 1%) such that could not be reproduced by the numerical simulations. This oil drag is due to the presence of drops with a smaller diameter than what was considered in this study. These drops are formed in the nozzle as a result of high speeds and cannot be separated by this process.

Figure 5 presents the comparison of images obtained from numerical simulations and experiments for v_m 0.25 m/s, 75 % water content in mixture and S = 0.6. The images on the left correspond to the top portion of the vertical cylinder, while the ones on the right correspond to the injection area. There is good agreement with respect to the distribution of each phase (water and oil) between the results from numerical simulations and experiments. The bottom part of the vertical cylinder was oil-free for the numerical simulations and the experiments.

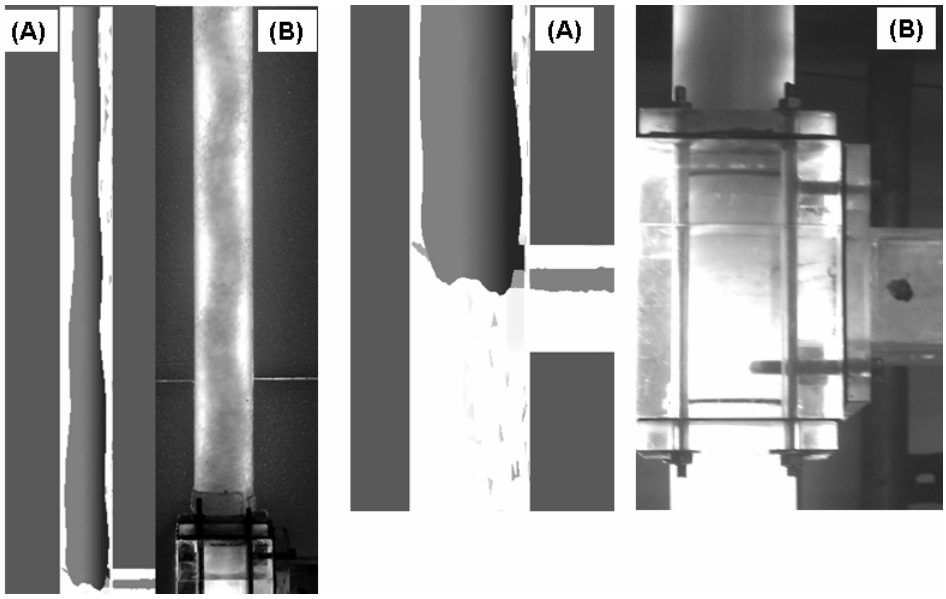

Figure 5. Phase distribution comparison for v_m = 0.25 m/s, wc = 75 % and S = 0.6. Left: top portion of the vertical cylinder; Right: injection area. (A) Numerical Solution and (B) Experiments.

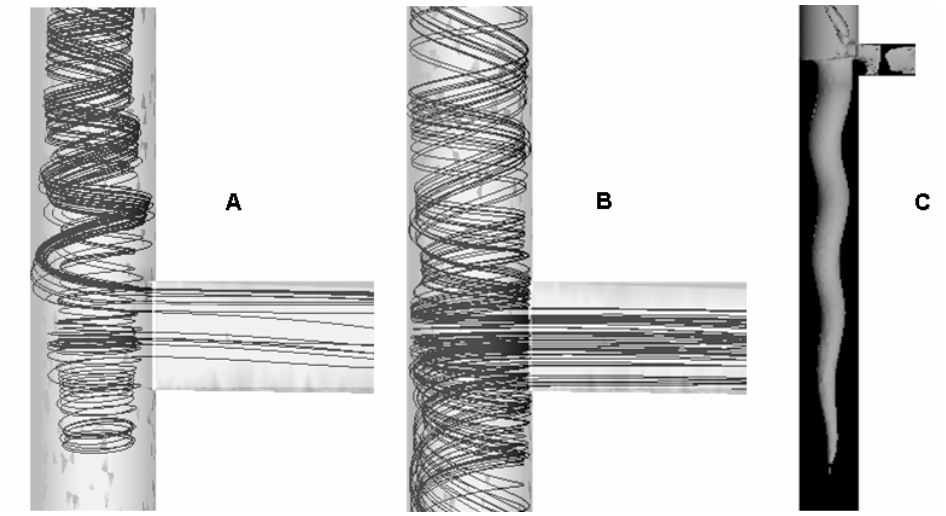

Figure 6. (A) Oil streamlines, (B) water streamlines and (C) capturing surface. All figures for v_m = 0.25 m/s, wc = 75% and S = 0.6

The basic working principle of the device can be observed by looking at the streamlines of each phase showed on Fig. 6. This figure shows three different plots: oil streamlines (A), water streamlines (B) and the capturing surface (C), all of them for v_m of 0.25 m/s, wc of 75% and S of 0.6. The capturing surface is obtained by plotting the points with zero vertical velocity. Points outside of the capturing surface will descend while points inside of it will ascend. The oil streamlines show that the fluid moves mainly in ascending direction and towards the center of the vertical cylinder. A small portion of the oil is dragged downwards but it ascends once it reaches the capturing surface. Water streamlines are located near the wall with a distribution that is dependent on the split ratio.

CONCLUSIONS

A fluid dynamic study of LLCC separators was conducted through numerical simulations and experiments. The results showed that numerical simulations performed under ANSYS-CFX 5.6™ were able to reproduce the separation capability of the LLCC separator for a wide range of operational conditions. The numerical results were obtained using a single drop diameter, which was fitted empirically. The plots of each phase distribution obtained through numerical simulations agree with the images acquired from the experiments. CFD tools can contribute significantly to the understanding of the multiphase flow inside the separator, thus contributing to the development of simpler models that can improve the design and operation of these devices.

ACKONWLEDGEMENTS

This work has been supported by FONACIT under grant G-2000001286 and by the DID from Universidad Simón Bolívar under grant S1-CA-015-04.

REFERENCES

1. Shoham, O. and G.E. Kouba, *State of the art of gas/liquid cylindrical-cyclone compact-separator technology.* Journal of Petroleum Technology, 1998. **50**(7): p. 58-65.
2. Gomez, L.E., et al., *Enhanced mechanistic model and field application design of gas/liquid cylindrical cyclone separators.* Spe Journal, 2000. **5**(2): p. 190-198.
3. Erdal, F.M., et al., *CFD simulation of single-phase and two-phase flow in Gas-Liquid Cylindrical Cyclone separators.* SPE Journal, 1997. **2**(4): p. 436-445.
4. Erdal, F.M. and S.A. Shirazi, *Local velocity measurements and computational fluid dynamics (CFD) simulations of swirling flow in a cylindrical cyclone.* Journal of Energy Resources Technology-Transactions of the Asme, 2004. **126**(4): p. 326-333.
5. Gomez, C., et al., *Oil/water separation in liquid/liquid hydrocyclones (LLHC): Part 1 - Experimental investigation.* Spe Journal, 2002. **7**(4): p. 353-361.
6. Caldentey, J., et al., *Oil/water separation in liquid/liquid hydrocyclones (LLHC): Part 2 - Mechanistic modeling.* Spe Journal, 2002. **7**(4): p. 362-372.
7. Mathiravedu, R., et al. *Performance and Control of Liquid-Liquid Cylindrical Cyclone Separators*. in *ASME Engineering Technology Conference on Energy*. 2002. Houston, Texas.
8. Oropeza-Vazquez, C., et al., *Oil-water separation in a novel liquid-liquid cylindrical cyclone (LLCC (c)) compact separator - Experiments and modeling.* Journal of Fluids Engineering-Transactions of the Asme, 2004. **126**(4): p. 553-564.
9. Ansys, *Reference Guide CFX 5.6*, in *http://www.ansys.com/cfx*. 2003.
10. Reyes-Gutiérrez, M.A., et al. *Eulerian-eulerian modeling of disperse two-phase flow in a gas-liquid cylindrical cyclone*. in *Proceedings of the ASME Heat Transfer/Fluids Engineering Summer Conference 2004, HT/FED 2004*. 2004
11. Panagiota, A., Geoffrey, H. *Drop size distributions in horizontal oil-water dispersed flow.* Chemical Engineering Science, 2000.**55**:p. 3133-3143.